40 Hz Auditory Steady-State Responses Predict Transition to Psychosis in Clinical-High-Risk Participants: A MEG Study

Grent-'t-Jong, Tineke, Ph.D.,[1,7] Gajwani, Ruchika, Ph.D.,[2] Gross, Joachim, Ph.D.,[1,3] Gumley, Andrew, I., Ph.D.,[2] Krishnadas, Rajeev, M.D., Ph.D.,[1] Lawrie, Stephen M., M.D.[4], Schwannauer, Matthias, Ph.D.,[5] Schultze-Lutter, Frauke., Ph.D.[6] & Uhlhaas, Peter J., Ph.D.[1,7]

1. Institute of Neuroscience and Psychology, University of Glasgow, Glasgow, U.K.
2. Mental Health and Wellbeing, Institute of Health and Wellbeing, University of Glasgow, Glasgow, U.K.
3. Institute for Biomagnetism and Biosignalanalysis, University of Muenster, Muenster, Germany
4. Department of Psychiatry, University of Edinburgh, Edinburgh, U.K.
5. Department of Clinical Psychology, University of Edinburgh, Edinburgh, U.K.
6. Department of Psychiatry and Psychotherapy, Medical Faculty, Heinrich Heine University Düsseldorf, Germany
7. Department of Child and Adolescent Psychiatry, Charité Universitätsmedizin, Berlin, Germany

Correspondence:

Prof. Peter J. Uhlhaas

Department of Child and Adolescent Psychiatry

Augustenburger Platz 1

Charité Universitätsmedizin

Berlin 13353

Germany

Email: peter.uhlhaas@charite.de

Tel: +49 30 450 516 193

Abstract

Objective: To examine whether 40-Hz Auditory Steady-State Responses (ASSR) in participants at clinical high-risk for psychosis predict clinical outcomes.

Method: In this study, magnetoencephalography (MEG) data were collected during a 40-Hz ASSR paradigm in 116 participants meeting clinical high-risk (CHR-P) for psychosis criteria, a clinical control group characterized by affective disorders and/or substance abuse (CHR-N: n=38), 32 first-episode psychosis patients (FEP, 14 antipsychotic-naïve), and 49 healthy controls. We examined 40-Hz-ASSR- source-activity in bilateral Heschl's gyrus, superior temporal gyrus, Rolandic operculum, and the thalamus. Group differences in ASSR amplitudes were tested and correlated with neuropsychological scores, psychosocial functioning, and clinical symptoms. Linear discriminant analyses was used to assess whether 40-Hz-ASSR predicts transition to psychosis and persistence of APS.

Results: Compared to controls, 40-Hz-ASSR responses in CHR-Ps were impaired in right Rolandic operculum (d=0.41) and right thalamus (d=0.43), particularly in those with combined UHR/BS symptoms and CHR-Ps who transitioned to psychosis (n=11). FEP-patients showed significant impairments in the right thalamus (d=0.58), while the CHR-N group was unaffected. Importantly, right thalamus 40-Hz-ASSRs predicted transition to psychosis (transitioned [n=11] vs non-transitioned [n=105]); classification accuracy 73.3%, AUC=0.827), whereas this was not the case for persistent APS (Persistent [n=41] vs non-Persistent [n=37]; classification accuracy 56.4%).

Conclusions: The current study indicates that MEG-recorded 40-Hz-ASSRs constitute a potential biomarker for predicting transition to psychosis in CHR-P participants.

Introduction

The brain's endogenous rhythmic activity represents a fundamental feature of large-scale circuits that has been implicated in cognition and behavior as well as in mental disorders, such as schizophrenia (1). One way to probe neural oscillations is through entrainment by exogenous sources, such as visual or auditory stimuli or brain stimulation (2). Current theories suggest that exogenous entrainment interacts with ongoing oscillatory of neural circuits that could provide possible treatment targets for brain disorders (3).

The Auditory Steady-State Response (ASSR) is an evoked oscillation that is entrained to the frequency and phase of temporally modulated auditory stimuli . ASSRs typically show a peak frequency at around 40 Hz, suggesting an auditory "resonant" frequency induced by external periodic stimulation (4). Magnetoencephalography (MEG), Positron Emission Tomography and functional Magnetic Resonance Imaging studies located the generators of the 40-Hz-ASSR in medial areas of the primary auditory cortex that are distinct from those underlying transient auditory components (5), as well as in thalamic and brainstem regions (6, 7).

One important application of the 40-Hz-ASSR has been in schizophrenia research because of the potential importance of gamma-band (30-200 Hz) oscillations in explaining cognitive deficits in the disorder (8). Gamma-band oscillations have been hypothesized to establish communication between distributed neuronal ensembles (9) and their impairment to underlie the pronounced cognitive and perceptual alterations in patients with schizophrenia (10). This view is consistent with data indicating that rhythm-generating parvalbumin-positive (PV+) γ-aminobutyric acid (GABA) interneurons and N-methyl-d-aspartate (NMDA) receptors are dysfunctional in schizophrenia (11), highlighting the potential of using noninvasively measured gamma-band oscillations to provide insights into circuit abnormalities in this disorder.

Currently, there is robust evidence that both amplitude and phase of 40-Hz-ASSR is impaired in schizophrenia (12, 13). There is mixed evidence, however, for the presence of 40-Hz-ASSRs deficits in both clinical high risk for psychosis (CHR-P) individuals (14, 15) and patients with first-episode psychosis (FEP) (16). Accordingly, it is currently unclear whether 40-Hz-ASSRs could also constitute a possible biomarker for the early detection and diagnosis of emerging psychosis.

To address this fundamental question, we applied a state-of-the-art MEG approach to examine 40-Hz-ASSRs in CHR-P participants, FEP-patients as well as clinical controls with substance-related and affective disorders (CHR-N). MEG is characterized by an improved signal-to-noise ratio for measurements of high-frequency oscillations compared to electroencephalography (EEG) . In addition, as MEG-data is ideally suited for source-reconstruction , we defined regions-of-interest (ROIs) in auditory cortex and the thalamus to reconstruct virtual channel-data of the 40-Hz-ASSR.

We predicted that FEP and CHR-P participants would be characterized by a circumscribed dysfunction of 40-Hz-ASSRs in auditory and thalamic regions that would be linked to clinical outcomes. Specifically, we hypothesized that impaired 40-Hz-ASSRs would predict persistence of attenuated psychotic symptoms (APS) as well as transition to psychosis in CHR-P participants.

METHOD

Participants

A total of 235 participants were recruited into the ongoing Youth Mental Health Risk and Resilience (YouR) Study (17) and divided into four groups: 1) 116 participants meeting CHR-P criteria, (2) 38 participants not meeting CHR-P criteria (CHR-N) but characterized by non-psychotic disorders, such as affective disorders (n=11), anxiety disorders (n=16), eating disorders (n=1), and/or substance abuse (n=10), 3) 32 patients with established FEP (14 antipsychotic-naïve) and, 4) 49 healthy control participants (HC) without an axis I diagnosis or family history of psychotic disorders.

CHR-P status at baseline was established by ultra-high risk criteria according to the Comprehensive Assessment of At Risk Mental States (CAARMS) Interview (18) and the Cognitive Disturbances (COGDIS) and Cognitive-Perceptive (COPER) basic symptoms criteria according to the Schizophrenia Proneness Instrument, Adult version (SPI-A) (19). FEP patients were assessed with the Structured Clinical Interview for DSM-IV (SCID) (see Table 1) (20) and with the Positive and Negative Symptom Scale (PANSS) (21). For all groups except FEP-patients, cognition was assessed with the Brief Assessment of Cognition in Schizophrenia (BACS) (22).

The study was approved by the ethical committees of University of Glasgow and the NHS Research Ethical Committee Glasgow & Greater Clyde. All participants provided written informed consent.

Clinical Follow-Up

Participants meeting CHR-P criteria were re-assessed at 3, 6, 9, 12, 18, 24, 30, and 36 months intervals (see also Online Supplement) to examine persistence of UHR criteria and transition to psychosis. Persistence of CHR-P criteria was operationalized by APS up to 12 months in this study. Criteria for transition to psychosis were defined on the basis of the CAARMS symptom scores of sufficient duration and frequency, using symptom severity and frequency scores. When transition to psychosis was confirmed, a SCID Interview was conducted to establish the DSM-IV-category of the psychotic disorder.

Stimuli and task

Auditory stimuli were 1000 Hz carrier tones of 2 seconds duration, presented binaurally through inner-ear tubes, with an inter-stimulus-interval of on average 2 seconds (jittered between 1.5 and 2.5 seconds, equal distribution). Participants were instructed to fixate a translucent screen (viewing distance: 75 cm). Participants received one block of 100 modulated tones at 40 Hz ('ripple tones', see Figure 1). To control for potential attentional differences, ten additional identical sounds with equal intensity levels over time ('flat tones') were interspersed, serving as targets to respond to by button-press.

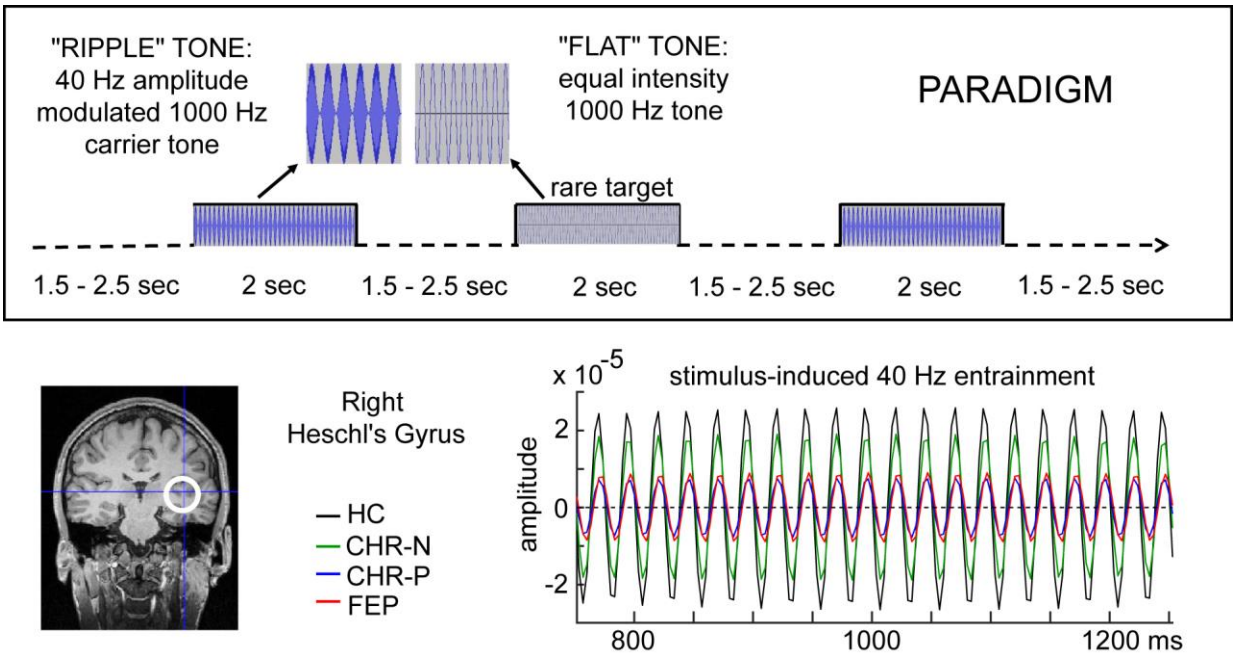

Figure 1: Task paradigm and example 40 Hz entrainment signal from the right primary auditory cortex (Heschl's gyrus).

Abbrev.: HC = healthy controls, CHR-N = clinical-high-risk negative clinical controls, CHR-P = clinical-high-risk positive, FEP = first-episode psychosis patients.

Neuroimaging

MEG-data were acquired from a 248-channel 4D-BTI magnetometer system (MAGNES® 3600 WH, 4D-Neuroimaging, San Diego), recorded with 1017.25 Hz sampling rate, and DC-400 Hz online filtered. T1 anatomical scans (3D MPRAGE sequences) were collected on a Siemens Trio Tim 3T-scanner (192 slices, voxel size 1 mm^3, FOV=256x256x176 mm^3, TR=2250 ms, TE=2.6 ms, FA=9°) for subject-specific source localization of MEG activity.

Task performance data analysis

Analysis of task data included computing percentage of correctly detected flat-tone targets (hit rate), errors (False Alarm rate), and mean reaction times (RT) of correct responses.

MEG data analysis

MEG data were analysed with MATLAB 2013b using the open-source Fieldtrip Toolbox Version 20161023 (http://www.fieldtriptoolbox.org/). Epochs of 4 seconds duration (1 second baseline), time-locked to sound onset, were extracted for the task-irrelevant 40-Hz amplitude-modulated tones only (excluding any with false alarm responses). Contamination of line noise was attenuated with a discrete 50-Hz Fourier transform filter. Faulty sensors with large signal variance or flat signals were removed, and the data down-sampled to 300 Hz. Artefact-free data were created by removing trials with excessive transient muscle activity, slow drift or SQUID jumps using visual inspection and Independent Component Analysis (ICA)-based removal of eye-blink, eye-movement and Electrocardiographic (ECG) artefacts.

The main analyses focused on data transformed into source space because regional specificity at each sensor is compromised by field-spread through inputs from multiple sources . In addition, inter-individual differences in temporal cortex folding creates large variance in source projections to the scalp of auditory-cortex activity. Based on prior findings (7, 23), source-analyses of the 40-Hz-ASSRs were restricted to a subset of four bilateral regions, defined in the AAL-atlas (24) as Heschl's gyrus (HES), Superior Temporal Gyrus (STG), Rolandic Operculum (ROL), and the Thalamus (THA).

MEG data were first co-registered with the participant's T1 scan, using anatomical landmarks (nasion, left and right pre-auricular points) and head-shape data collected using a Polhemus 3D Fasttrack digitization system prior to recordings. Subsequently, a three-dimensional grid of 5 mm resolution was created and linearly warped into a single-shell volume conductor model, created from the segmented T1 scan data. Virtual channel time-series data were then computed using LCMV beamformers (25), with normalized lead-fields and a regularisation parameter of 20% to attenuate leakage from nearby sources. These virtual-channel time-series were computed separately for each voxel within each of the ROIs (bilateral HES, STG, ROL and THA, see

Figure 2), and then combined into one time-series per ROI, using the first component from a Singular Value Decomposition (SVD) analysis of the single-voxel data.

40-Hz-ASSR responses were extracted by band-pass filtering single-trial virtual-channel data with a sharp Butterworth filter (range 39.6-40.4 Hz, two-pass, roll-off = 4, see Figure 1). Data were subsequently Hilbert transformed and averaged across trials. Data were then normalised for each participant by subtracting the mean of the baseline activity (-500-0 ms) from each time-point and dividing the values across the entire epoch by the baseline data (relative change).

Statistical analyses

Group comparisons

Group differences in trial numbers, task performance, demographic and clinical data were assessed with non-parametric Kruskal-Wallis tests, alpha-level 0.05, 2-sided, with post-hoc pairwise comparisons Bonferroni-corrected for Type I errors. BACS data were first z-normalized to the HC data. Sex differences were tested with Chi-Square tests.

In order to estimate statistical group differences in virtual-channel 40-Hz-ASSR activity, mean 40-Hz-ASSR activity from each of the eight ROIs (0-2000 ms, relative change from baseline) and each subject within the four main groups (HC, CHR-N, CHR-P, and FEP) were log10 transformed (to create normal distributions) and subjected to a non-parametric permutation (n=5000) t-test, tested against the null hypothesis of no difference from the HC group, using estimation statistics (26). Confidence intervals (CI) were obtained from the central 95% of the resampling distribution. To account for skewed data distribution, data were bias and accelerated bootstrap corrected.

Separate analyses were conducted on CHR-P subgroups (Basic Symptoms [BS] only, attenuated psychotic symptoms [UHR] only, combined UHR/BS). In addition, CHR-P participants with persistent APS (APS-P) vs. non-persistent APS (APS-NP) within 1-year follow-up as well as participants who transitioned to psychosis (CHR-P-T) vs those who did not (CHR-P-NT) were examined.

Correlational analyses

For the CHR-P group, correlations with clinical variables at baseline (CAARMS severity, SPI-A severity, General Assessment of Functioning [GAF] score, Global Functioning role and social scores, CHR subgroup [BS only, UHR only, or combined UHR/BS], SPI-A category [COGDIS, COPER, both criteria]), and cognitive variables at baseline (BACS composite score) were tested using linear regression models (alpha 0.05, 2-sided, 1000 sample bootstrapping), with the ROI-specific 40-Hz-ASSR activity as dependent variables.

Classification analyses

We used Linear Discriminant Analysis to evaluate whether 40-Hz-ASSR impairments uniquely contributed towards APS persistence and/or transitioning to psychosis. For APS persistence, a persistent (APS-P, n=41) group and a non-persistent group of CHR-P participants (APS-NP, n=37) were modeled using significant 40-Hz-ASSR activity alone, significantly impaired clinical/functional data alone, or a combination of all predictors. Data were cross-validated with a leave-one-out method. For each model, both Wilks' Lambda/Chi-Square tests as well as area under the Receiver Operating Characteristic Curve (AUC) were evaluated. A similar strategy was used to evaluate models for classifying transitioned CHR-Ps (CHR-P-T, n=11) vs. non-transitioned individuals (CHR-P-NT, n=105).

Results

Demographic Data and ASSR-Task performance

The FEP group included significantly more male participants compared to HC ($\chi^2(1)=8.5$, p=0.004), CHR-N ($\chi^2(1)=9.4$, p=0.002) and CHR-P groups ($\chi^2(1)=14.1$, p<0.001) (Table 1). The BACS composite score was significantly lower in CHR-P participants compared to HC (-0.61; 95% CI, -0.99 to -0.25, p<0.001). FEP, CHR-P and CHR-N had significantly lower Global Assessment of Functioning (GAF) scores than HC participants (CHR-N, -18; 95% CI, -22 to -13; p<0.001; CHR-P, -30; 95% CI, -33 to -27 ; p<0.001; FEP, -49; 95% CI, -44 to -54; p<0.001). The CHR-P group scored lower than HC in global role (CHR-P, -1.18, 95% CI, -1.55 to -0.81, p<0.001) and both CHR-P and CHR-N also in social functioning (CHR-N, -0.63, 95% CI, -0.99 to -0.28, p=0.003; CHR-P, -1.38, 95% CI, -1.68 to -1.07, p<0.001). There were no main group differences (Table 1) in behavioral performance on rare targets.

Follow-Up Outcomes

We examined persistence of APS within a 12 months follow-up period in CHR-P participants that met APS-criteria at baseline (n=86, 74.1%). For 78 CHR-P participants (67.2%), at least one follow-up assessment within one year was available and 41 CHR-Ps continued to meet APS-criteria (Table S3, Online Supplement). Compared to APS-NP group, the APS-P group scored significantly higher on CAARMS and SPI-A severity as well as significantly lower on GF-role at baseline (Table S2, Online Supplement).

Eleven (9.5 %) out of the 116 CHR-P participants (9 met APS-P group) made a transition to psychosis (CHR-P-T group; mean follow-up period 18 months [6-36 months], see further sample characteristics, including SCID diagnosis, Table 3 of Online Supplement).

40-Hz-ASSR Main Group Results

A robust 40-Hz entrainment signal in primary auditory cortex (i.e., right Heschl's gyrus) was observed for all groups (Figure 1, lower panel), with HC and CHR-N groups showing the largest response. Compared to HC (Figure 2), the 40-Hz-ASSR amplitude in the RROL was significantly reduced in the CHR-P group (-0.13,

95% CI: -0.24 to -0.02, p=0.02, d=0.41), and significantly lower amplitudes were found in the RTHA for both the CHR-P group (-0.14, 95% CI: -0.26 to -0.015, p=0.026, d=0.43) and the FEP patients (-0.23, 95% CI: -0.40 to -0.05, p=0.013, d=0.58). No impairments were found for CHR-N participants.

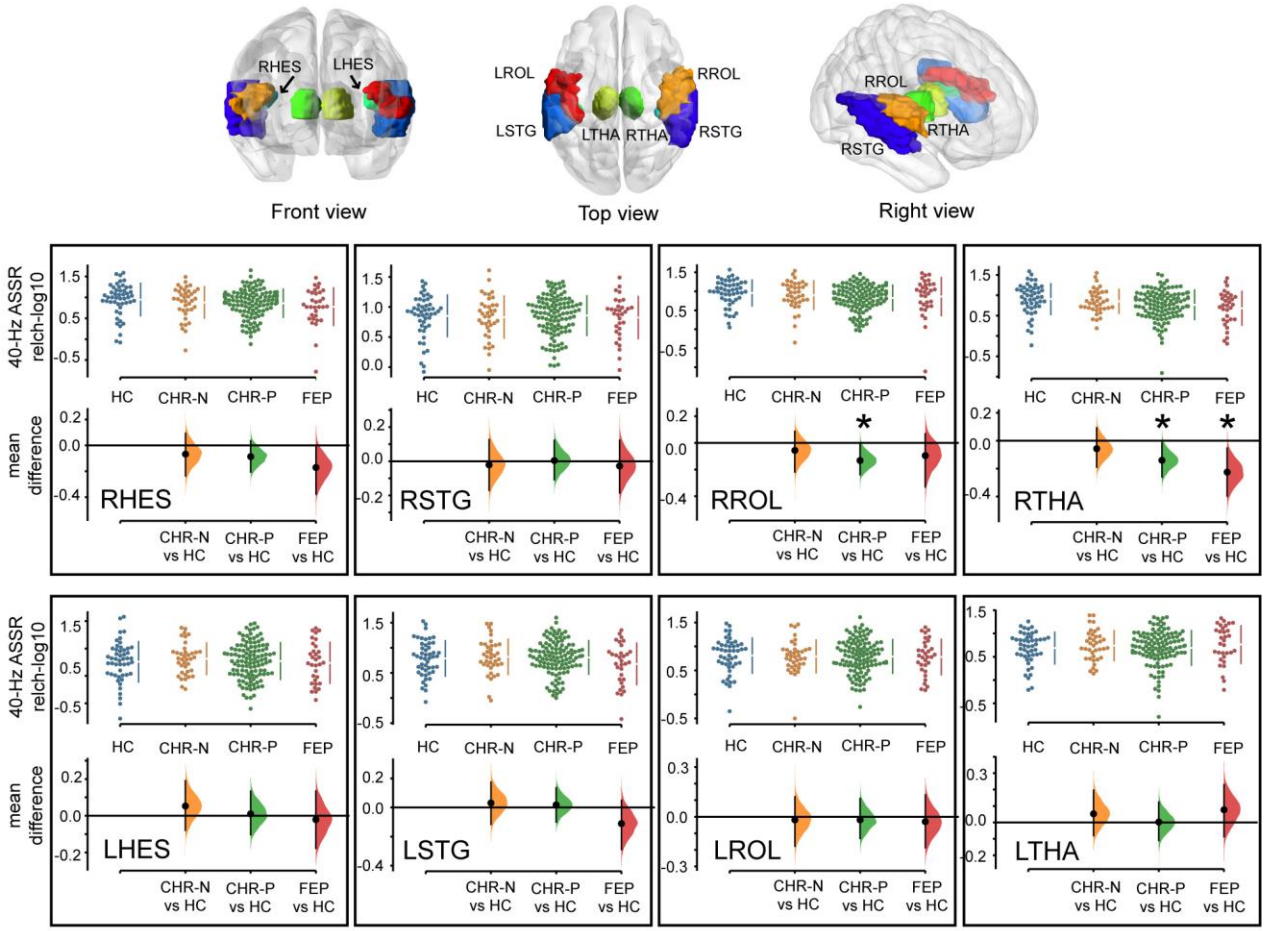

Figure 2. Main group differences in the 40-Hz ASSR amplitude.

Top panel shows the locations of the eight tested ROIs, including bilateral HES, STG, ROL and THA. Bottom row figures show Cumming Estimation Plots with data distribution swarm plots and group difference data distributions (compared to healthy controls) for all eight investigated ROIs. Two ROIs, the RROL and RTHA areas (middle panel, two most right figures), showed significant impairments ($p < 0.05$) in 40-Hz ASSR response in CHR-P and/or FEP group, compared to control individuals (indicated by an *). Abbrev.: HC = healthy controls, CHR-N = clinical-high-risk negative, CHR-P = clinical-high-risk positive, FEP = First-Episode Psychosis.

40-Hz-ASSR Impairments in CHR-P Subgroups

We additionally investigated CHR-P subgroups for the two ROIs with main group effects (RROL and RTHA: Figure 2 and 3); 1) BS only (n=30), UHR only (n=31), and combined UHR/BS group (n=55), 2) CHR-P

participants with persistent (APS-P: n=41) and remitted APS (APS-NP: n=37), and 3) transitioned CHR-P-T (n=11) and non-transitioned CHR-P-NT (n=105).

Impairments in 40-Hz-ASSR in the RROL area were found for the UHR/BS group (-0.14, 95% CI: -0.26 to -0.004, p=0.047, d=0.41), the persistent APS-P group (-0.15, 95% CI: -0.29 to -0.008, p=0.047, d=0.43), and non-transitioned CHR-Ps (CHR-P-NT: -0.13, 95% CI: -0.24 to -0.013, p=0.027, d=0.38) compared to HC. Impairments in the RTHA were present in the UHR/BS group (-0.14, 95% CI: -0.27 to -0.008, p=0.035, d=0.43), the persistent APS-P group (-0.20, 95% CI: -0.34 to -0.05, p=0.008, d=0.55), and the transitioned CHR-P-T group (-0.36, 95% CI: -0.56 to -0.15, p=0.004, d=1.14).

The transitioned group (CHR-P-T) was also significantly more impaired than the non-transitioned group (CHR-P-NT) in the RTHA (-0.26, 95% CI: -0.44 to -0.09, p=0.024, d=0.80) but not in the RROL area (-0.04, 95% CI: -0.23 to -0.12, p=0.75, d=0.13).

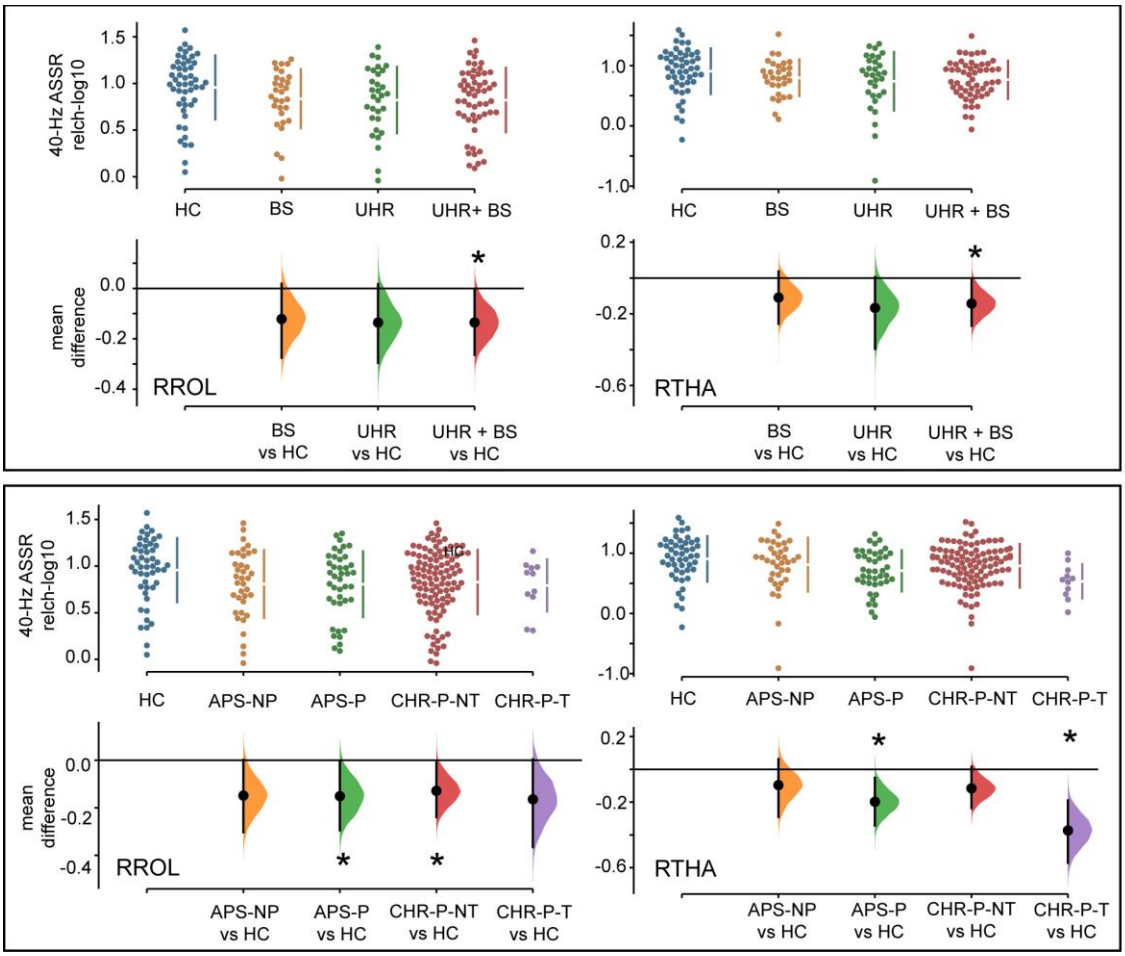

Figure 3. 40-Hz ASSR Amplitude Impairments in CHR-P Subgroups

Cumming Estimation Plots of RROL (left plots) and RTHA (right plots) data with indicated significance (*) from healthy controls (HC). Top row shows data from for CHR-P subgroups based on meeting UHR symptom and/or basic symptom (BS) threshold criteria at baseline. Bottom row figures show data from follow-up based group divisions, with either presence (APS-P) or absence

of persistence of attenuated psychotic symptoms (APS-NP) up to 1 year follow-up assessment, or based on having transitioned to psychosis (CHR-P-T) or not (CHR-P-NT). Abbrev.: SPI-A = Schizophrenia Proneness Instrument, Adult version, CAARMS = Comprehensive Assessment of At-Risk Mental States, APS = attenuated psychotic symptoms.

Medication Effects in the FEP Group

Compared to HCs, significant impairments in the RTHA were evident only in FEP-patients that were on antipsychotic medication (n=18; -0.22, 95% CI: -0.39 to -0.04, p=0.032, d=0.62). There were, however, no differences between medicated and un-medicated FEP patients (Figure S3, Online Supplement).

Correlations

We did not find any significant correlations between 40-Hz-ASSRs and demographic, clinical, or neuropsychological parameters in the CHR-P group (n=116).

Baseline differences

We additionally tested baseline activity of significant ROIs for potential 40-Hz group differences. No significant group differences were observed (See Figure S1 in Online Supplement).

Classification of APS-Persistence and Transition in the CHR-P Group

We evaluated the contribution of impaired RTHA 40-Hz-ASSR activity to both persistence of APS (Persistent [APS-P, n=41] vs. non-Persistent [APS-NP, n=37]), as well as predicting transitioning to psychosis (Transitioned [CHR-P-T, n=11] vs. non-Transitioned [CHR-P-NT, n=105]), using Linear Discriminant Analyses. Classification performance for separating APS-P from APS-NP individuals was poor (Table 2: 55.1-56.4%, AUC = 0.602-0.661) for all three models; neural data (RTHA) alone, clinical data (GF-role, SPI-A severity) alone and in combination. In contrast, a good model was found based on RTHA 40-Hz activity alone for classifying transitioned CHR-P-T vs. non-transitioned CHR-P-NT individuals (81.8% for transitioned cases). The addition of GAF and GF-social scores to the model resulted in the highest overall classification accuracy (Tabel 2: 73.3%, ROC-AUC = 0.827).

MEG activity in Thalamus

To examine potential source-leakage from cortical sources and/or effects of depth-bias corrections implemented in the source-estimation algorithm, we additionally tested for any group differences in other subcortical structures, including bilateral putamen, caudate and pallidum, to validate the RTHA results. None of the addition regions showed significant group differences (Figure S2, Online Supplement).

Discussion

Robust evidence exists for impairments in the 40-Hz-ASSR in ScZ-patients (12). This is consistent with evidence for alterations in neural circuits that are involved in the generation of gamma-band rhythms, such as the PV+ interneurons and NMDA-R mediated neurotransmission (11). However, it is currently unknown whether the 40-Hz-ASSR is impaired during emerging psychosis and thus could potentially constitute a biomarker for early diagnosis and detection of psychosis. To address this fundamental issue, we implemented a state-of-the-art MEG-approach to examine the 40-Hz-ASSR in auditory and thalamic areas in a large CHR-P sample to determine whether we could predict persistence of APS-status and transition to psychosis.

Consistent with our hypothesis, we found a reduction in 40-Hz-ASSR amplitudes in both FEP and CHR-P participants in auditory and thalamic regions. This contrasts with several recent EEG-studies that found intact 40-Hz-ASSRs in both CHR-P (27) and FEP-groups (28). One possible explanation are differences in recording techniques of 40-Hz-ASSRs. MEG is characterized by an increased-signal-to-noise ratio compared to EEG for the measurement of high-frequency oscillations . In addition, we implemented a novel analysis approach that involved band-pass filtering of single-trial MEG-activity in combination with virtual-channel data that may have facilitated the detection of 40-Hz-ASSR-impairments in CHR-P and FEP-groups.

In terms of the location of 40-Hz-ASSR impairments, we found reductions in both RROL and RTHA in CHR-P participants, while deficits in the FEP-group were confined to the RTHA. These findings contrast with previous observations in ScZ that have localized 40-Hz-ASSR deficits to primary auditory cortex (Heschl's gyrus) and/or the superior temporal cortex (29, 30). Accordingly, our data highlight that impairments in the 40-Hz-ASSR during emerging psychosis may involve higher auditory areas as well as contributions from thalamic sources while impairments in primary auditory regions may emerge during later illness stages.

A key finding from our study is that reductions in 40-Hz-ASSRs have prognostic significance in CHR-P participants. Specifically, we found that 40-Hz-ASSR in the thalamus predicted transition to psychosis. These are the first findings suggesting that gamma-band oscillations could have potential as a biomarker in CHR-P participants, which is a critical finding since only a minority of CHR-P participants will develop psychosis (31) and a large number of individuals will remit from CHR-P status (32). Interestingly, 40-Hz-ASSR

impairments only predicted in combination with measures of functioning persistence of APS-symptoms at 12-months.

In addition, we also found that reductions in the 40-Hz-ASSRs were pronounced in CHR-P participants that met UHR/BS criteria. Previous studies have shown that CHR-P participants with a combination of both APS/UHR and BS were characterized by increased transition rates (33) and elevated psychopathology (34). Accordingly, these findings suggest that 40-Hz-ASSRs may be a biomarker for addressing the significant clinical heterogeneity of the CHR-P phenotype.

The significant contribution of the thalamus towards 40-Hz-ASSR deficits in both CHR-P and FEP-groups is consistent with several lines of evidence: Firstly, during normal brain functioning, thalamic 40-Hz-ASSRs have been observed with several neuroimaging approaches, including PET, fMRI and EEG/MEG (6, 7, 23). Furthermore, experimentally induced thalamic evoked gamma oscillations have a direct effect on auditory cortex ASSR responses to click trains (35). Secondly, abnormal thalamic activity and their interactions with cortical and sub-cortical structures have recently emerged as possible key contributor towards the emergence of psychosis (36). In addition, oxidative stress, a key pathophysiological process implicated in developing psychosis, targets specifically the thalamic reticular nucleus by reducing PV-interneurons and related gamma-band activity (37).

Finally, we did not find 40-Hz-ASSR impairments in CHR-N individuals, suggesting that impaired gamma-band oscillations are specifically associated with the CHR-P and FEP phenotypes. We could also exclude the possibility that 40-Hz-ASSR impairments in FEP-patients were the result of antipsychotic medication since medicated FEP-patients did not differ significantly in 40-Hz amplitudes from non-medicated patients.

Strengths and Limitations

There are a several limitations of the current study. Firstly, we used a novel different analysis approach that did not include examination of differences in inter-trial phase-coherence. Secondly, we localized the most consistent differences to the thalamus. While localization of thalamic generators from MEG data remains challenging, we would like to note that reconstruction of MEG time-courses in the thalamus has been consistently demonstrated by our (38, 39) and other groups (40). Moreover, our analyses revealed that there

were no differences in neighboring structures, such as putamen, pallidum and caudate nucleus, suggesting that signal-leakage, for example, did not contribute to our observations. Finally, the sample size of CHR-P-T was relatively small (n=11) although effect sizes in this group were large and their data consistent enough to predict psychosis development with moderately high accuracy. Nonetheless, the current findings need be replicated in a larger sample of CHR-P participants.

In conclusion, the current study provides novel evidence on the presence of 40-Hz-ASSRs deficits in CHR-P participants and FEP-patients and the associated brain regions that give rise to this impairment. Crucially, the current findings highlight that MEG-measured gamma-band oscillations in CHR-P participants predict transition to psychosis, highlighting the possibility that 40-Hz-ASSRs constitute a potential biomarker for early detection and diagnosis of emerging psychosis.

Disclosures and acknowledgments

Dr. Uhlhaas has received research support from Lilly and Lundbeck outside the submitted work. Dr. Lawrie has received a personal fee from Sunovion outside the submitted work. The study was supported by the Medical Research Council (MR/L011689/1). Dr. Rajeev Krishnadas was supported by the Neurosciences Foundation.

We thank Frances Crabbe for help in the acquisition of MEG/MRI-data. The investigators also acknowledge the support of the Scottish Mental Health Research Network (http://www.smhrn.org.uk) now called the NHS Research Scotland Mental Health Network (NRS MHN: http://www.nhsresearchscotland.org.uk/research-areas/mental-health) for providing assistance with participant recruitment, interviews, and cognitive assessments. We would like to thank both the participants and patients who took part in the study and the research assistants of the YouR-study for supporting the recruitment and assessment of CHR-participants.

References

1. Uhlhaas PJ, Singer W. Abnormal neural oscillations and synchrony in schizophrenia. Nat Rev Neurosci. 2010;11:100-113.

2. Lakatos P, Gross J, Thut G. A New Unifying Account of the Roles of Neuronal Entrainment. Curr Biol. 2019;29:R890-R905.

3. Uhlhaas PJ, Singer W. Neuronal dynamics and neuropsychiatric disorders: toward a translational paradigm for dysfunctional large-scale networks. Neuron. 2012;75:963-980.

4. Ross B: Steady-state auditory evoked responses. Celesia GG, editor. Amsterdam: the Netherlands, Elsevier; 2013.

5. Draganova R, Ross B, Wollbrink A, Pantev C. Cortical steady-state responses to central and peripheral auditory beats. Cereb Cortex. 2008;18:1193-1200.

6. Reyes SA, Salvi RJ, Burkard RF, Coad ML, Wack DS, Galantowicz PJ, Lockwood AH. PET imaging of the 40 Hz auditory steady state response. Hear Res. 2004;194:73-80.

7. Steinmann I, Gutschalk A. Potential fMRI correlates of 40-Hz phase locking in primary auditory cortex, thalamus and midbrain. Neuroimage. 2011;54:495-504.

8. Uhlhaas PJ, Singer W. Neural synchrony in brain disorders: relevance for cognitive dysfunctions and pathophysiology. Neuron. 2006;52:155-168.

9. Fries P. Neuronal gamma-band synchronization as a fundamental process in cortical computation. Annu Rev Neurosci. 2009;32:209-224.

10. Spencer KM, Nestor PG, Niznikiewicz MA, Salisbury DF, Shenton ME, McCarley RW. Abnormal neural synchrony in schizophrenia. J Neurosci. 2003;23:7407-7411.

11. Sohal VS, Zhang F, Yizhar O, Deisseroth K. Parvalbumin neurons and gamma rhythms enhance cortical circuit performance. Nature. 2009;459:698-702.

12. Thune H, Recasens M, Uhlhaas PJ. The 40-Hz Auditory Steady-State Response in Patients With Schizophrenia: A Meta-analysis. JAMA Psychiatry. 2016;73:1145-1153.

13. Light GA, Hsu JL, Hsieh MH, Meyer-Gomes K, Sprock J, Swerdlow NR, Braff DL. Gamma band oscillations reveal neural network cortical coherence dysfunction in schizophrenia patients. Biol Psychiatry. 2006;60:1231-1240.

14. Koshiyama D, Kirihara K, Tada M, Nagai T, Fujioka M, Ichikawa E, Ohta K, Tani M, Tsuchiya M, Kanehara A, Morita K, Sawada K, Matsuoka J, Satomura Y, Koike S, Suga M, Araki T, Kasai K. Electrophysiological evidence for abnormal glutamate-GABA association following psychosis onset. Transl Psychiatry. 2018;8:211.

15. Tada M, Nagai T, Kirihara K, Koike S, Suga M, Araki T, Kobayashi T, Kasai K. Differential Alterations of Auditory Gamma Oscillatory Responses Between Pre-Onset High-Risk Individuals and First-Episode Schizophrenia. Cereb Cortex. 2016;26:1027-1035.

16. Spencer KM, Salisbury DF, Shenton ME, McCarley RW. Gamma-band auditory steady-state responses are impaired in first episode psychosis. Biol Psychiatry. 2008;64:369-375.

17. Uhlhaas PJ, Gajwani R, Gross J, Gumley AI, Lawrie SM, Schwannauer M. The Youth Mental Health Risk and Resilience Study (YouR-Study). BMC Psychiatry. 2017;17:43.

18. Yung AR, Yuen HP, McGorry PD, Phillips LJ, Kelly D, Dell'Olio M, Francey SM, Cosgrave EM, Killackey E, Stanford C, Godfrey K, Buckby J. Mapping the onset of psychosis: the Comprehensive Assessment of At-Risk Mental States. Aust N Z J Psychiatry. 2005;39:964-971.

19. Schultze-Lutter F, Addington, J., Ruhrmann, S., Klosterkötter, K. : SCHIZOPHRENIA PRONENESS INSTRUMENT, ADULT VERSION (SPI-A). Rome, Giovanni Fioriti Editore 2007.

20. First MB, Spitzer, R.L., Gibbon, M., Williams, J.B.W.,: Structured Clinical Interview for DSM IV Axis I Disorders—Patient Edition (SCID-I/P Version 2.0). New York, Biometrics Research Department, New York State Psychiatric Institute; 1995.

21. Kay SR, Fiszbein A, Opler LA. The positive and negative syndrome scale (PANSS) for schizophrenia. Schizophr Bull. 1987;13:261-276.

22. Keefe RS, Goldberg TE, Harvey PD, Gold JM, Poe MP, Coughenour L. The Brief Assessment of Cognition in Schizophrenia: reliability, sensitivity, and comparison with a standard neurocognitive battery. Schizophr Res. 2004;68:283-297.

23. Farahani ED, Goossens T, Wouters J, van Wieringen A. Spatiotemporal reconstruction of auditory steady-state responses to acoustic amplitude modulations: Potential sources beyond the auditory pathway. Neuroimage. 2017;148:240-253.

24. Tzourio-Mazoyer N, Landeau B, Papathanassiou D, Crivello F, Etard O, Delcroix N, Mazoyer B, Joliot M. Automated anatomical labeling of activations in SPM using a macroscopic anatomical parcellation of the MNI MRI single-subject brain. Neuroimage. 2002;15:273-289.

25. Van Veen BD, van Drongelen W, Yuchtman M, Suzuki A. Localization of brain electrical activity via linearly constrained minimum variance spatial filtering. IEEE Trans Biomed Eng. 1997;44:867-880.

26. Ho J, Tumkaya T, Aryal S, Choi H, Claridge-Chang A. Moving beyond P values: data analysis with estimation graphics. Nat Methods. 2019;16:565-566.

27. Lepock JR, Ahmed S, Mizrahi R, Gerritsen CJ, Maheandiran M, Drvaric L, Bagby RM, Korostil M, Light GA, Kiang M. Relationships between cognitive event-related brain potential measures in patients at clinical high risk for psychosis. Schizophr Res. 2019.

28. Bartolomeo LA, Wright AM, Ma RE, Hummer TA, Francis MM, Visco AC, Mehdiyoun NF, Bolbecker AR, Hetrick WP, Dydak U, Barnard J, O'Donnell BF, Breier A. Relationship of auditory electrophysiological responses to magnetic resonance spectroscopy metabolites in Early Phase Psychosis. Int J Psychophysiol. 2019;145:15-22.

29. Hamm JP, Bobilev AM, Hayrynen LK, Hudgens-Haney ME, Oliver WT, Parker DA, McDowell JE, Buckley PA, Clementz BA. Stimulus train duration but not attention moderates gamma-band entrainment abnormalities in schizophrenia. Schizophr Res. 2015;165:97-102.

30. Spencer KM, Niznikiewicz MA, Nestor PG, Shenton ME, McCarley RW. Left auditory cortex gamma synchronization and auditory hallucination symptoms in schizophrenia. BMC Neurosci. 2009;10:85.

31. Fusar-Poli P, Salazar de Pablo G, Correll CU, Meyer-Lindenberg A, Millan MJ, Borgwardt S, Galderisi S, Bechdolf A, Pfennig A, Kessing LV, van Amelsvoort T, Nieman DH, Domschke K, Krebs MO, Koutsouleris N, McGuire P, Do KQ, Arango C. Prevention of Psychosis: Advances in Detection, Prognosis, and Intervention. JAMA Psychiatry. 2020;77:755-765.

32. Simon AE, Borgwardt S, Riecher-Rossler A, Velthorst E, de Haan L, Fusar-Poli P. Moving beyond transition outcomes: meta-analysis of remission rates in individuals at high clinical risk for psychosis. Psychiatry Res. 2013;209:266-272.

33. Schultze-Lutter F, Klosterkotter J, Ruhrmann S. Improving the clinical prediction of psychosis by combining ultra-high risk criteria and cognitive basic symptoms. Schizophr Res. 2014;154:100-106.

34. Glenthoj LB, Bailey B, Kristensen TD, Wenneberg C, Hjorthoj C, Nordentoft M. Basic symptoms influence real-life functioning and symptoms in individuals at high risk for psychosis. Acta Psychiat Scand. 2020;141:231-240.

35. Sukov W, Barth DS. Cellular mechanisms of thalamically evoked gamma oscillations in auditory cortex. J Neurophysiol. 2001;85:1235-1245.

36. Anticevic A, Haut K, Murray JD, Repovs G, Yang GJ, Diehl C, McEwen SC, Bearden CE, Addington J, Goodyear B, Cadenhead KS, Mirzakhanian H, Cornblatt BA, Olvet D, Mathalon DH, McGlashan TH, Perkins DO, Belger A, Seidman LJ, Tsuang MT, van Erp TG, Walker EF, Hamann S, Woods SW, Qiu M, Cannon TD. Association of Thalamic Dysconnectivity and Conversion to Psychosis in Youth and Young Adults at Elevated Clinical Risk. JAMA Psychiatry. 2015;72:882-891.

37. Steullet P, Cabungcal JH, Bukhari SA, Ardelt MI, Pantazopoulos H, Hamati F, Salt TE, Cuenod M, Do KQ, Berretta S. The thalamic reticular nucleus in schizophrenia and bipolar disorder: role of parvalbumin-expressing neuron networks and oxidative stress. Mol Psychiatry. 2018;23:2057-2065.

38. Roux F, Wibral M, Singer W, Aru J, Uhlhaas PJ. The phase of thalamic alpha activity modulates cortical gamma-band activity: evidence from resting-state MEG recordings. J Neurosci. 2013;33:17827-17835.

39. Grent-'t-Jong T, Rivolta D, Gross J, Gajwani R, Lawrie SM, Schwannauer M, Heidegger T, Wibral M, Singer W, Sauer A, Scheller B, Uhlhaas PJ. Acute ketamine dysregulates task-related gamma-band oscillations in thalamo-cortical circuits in schizophrenia. Brain. 2018;141:2511-2526.

40. Attal Y, Bhattacharjee M, Yelnik J, Cottereau B, Lefevre J, Okada Y, Bardinet E, Chupin M, Baillet S. Modeling and detecting deep brain activity with MEG & EEG. Conf Proc IEEE Eng Med Biol Soc. 2007;2007:4937-4940.

Table 1. Demographics, Clinical Data, and Task Performance

	HC	CHR-N	CHR-P	FEP	Group effect [a]	Post-hoc comparisons
Number of participants	49	38	116	32		
Age: years (SD)	23 (3.6)	23 (4.7)	22 (4.5)	24 (4.5)		
Sex: male/female (% male)	16/33 (32.7)	11/27 (28.9)	34/82 (29.3)	21/11 (65.5)	$\chi(3) = 15.6$, $p = 0.001$	FEP > HC: $p = 0.004$
						FEP > CHR-N: $p = 0.002$
						FEP > CHR-P: $p < 0.001$
Education: years (SD)	17 (3.0)	16 (3.5)	15 (3.2)	15 (2.9)	$H(3) = 9.8$, $p = 0.021$	CHR-P < HC: $p = 0.032$
BACS [b]: mean (SD)						
Verbal memory	52 (8.7)	0.01 (1.1)	-0.36 (1.3)	NA		
Digit sequencing	21 (2.1)	0.14 (1.2)	-0.16 (1.5)	NA		
Token motor	81 (11.6)	-0.66 (1.1)	-1.01 (1.3)	NA	$H(2) = 20.7$, $p < 0.001$	CHR-P < HC: $p < 0.001$
Verbal fluency	59 (13.9)	-0.22 (1.0)	0.05 (1.3)	NA		
Symbol coding	74 (11.8)	0.00 (1.3)	-0.58 (1.1)	NA	$H(2) = 15.8$, $p < 0.001$	CHR-P < HC: $p = 0.002$
						CHR-P < CHR-N: $p = 0.013$
Tower of London	19 (1.7)	0.15 (1.3)	-0.15 (1.5)	NA		
Composite score	304 (24.2)	-0.15 (1.2)	-0.62 (1.4)	NA	$H(2) = 9.6$, $p = 0.008$	CHR-P < HC: $p = 0.014$
CAARMS scores: mean (SD)						
Unusual Thought Content	0 (0.1)	1 (1.2)	2 (2.0)	NA		
Non-bizarre Ideas	0 (0.4)	1 (1.1)	3 (1.8)	NA		
Perceptual Abnormalities	0 (0.5)	1 (1.3)	3 (1.5)	NA		
Disorganized Speech	0 (0.1)	1 (0.9)	1 (1.4)	NA		
Total severity score	1 (2.4)	6 (6.1)	30 (18.0)	NA	$H(2) = 125.2$, $p < 0.001$	CHR-N > HC: $p = 0.01$
						CHR-P > HC: $p < 0.001$
						CHR-P > CHR-N: $p < 0.001$
CHR-P categories: n (%)						
SPI-A (COGDIS/COPER/both items)	0	0	30 (26) (4 / 15 / 11)	NA		
CAARMS (APS- /GRFD-criteria [c])	0	0	31 (27) (29 / 2)	NA		
CAARMS + SPI-A (COGDIS / COPER / both items)	0	0	55 (47) (8 / 22 / 25)	NA		
SPI-A severity: mean (SD)	0	0	11 (11.6)	NA		
MINI categories [d]**:** n (%)						
Depressive/Mood disorders	0 (0)	11 (29)	75 (65)	NA		
Anxiety disorders/PTSD/OCD	0 (0)	16 (42)	85 (73)	NA		
Drug/alcohol abuse/dependence	2 (4)	10 (26)	39 (33)	NA		
Eating Disorders	0 (0)	1 (2)	9 (8)	NA		
GAF: mean (SD)	88 (6.4)	70 (12.8)	58 (13.8)	39 (13.9)	$H(2) = 139.5$, $p < 0.001$	All contrasts $p < 0.005$
GF-role: mean (SD)	8.6 (0.8)	8.1 (0.8)	7.4 (1.2)	NA	$H(2) = 50.5$, $p < 0.001$	CHR-P < HC: $p < 0.001$
						CHR-P < CHR-N: $p = 0.002$
GF-social: mean (SD)	8.8 (0.4)	8.2 (0.8)	7.4 (1.3)	NA	$H(2) = 62.0$, $p < 0.001$	CHR-N < HC: $p = 0.003$

						CHR-P < HC: p < 0.001
						CHR-P < CHR-N: p = 0.003
PANSS: mean (SD)						
Positive	NA	NA	NA	20 (8.0)		
Negative	NA	NA	NA	16 (9.2)		
Cognitive	NA	NA	NA	21 (9.3)		
Excitement	NA	NA	NA	9 (4.6)		
Depression	NA	NA	NA	11 (5.9)		
Total score	NA	NA	NA	77 (28.7)		
DSM-IV / SCID-IP						
Schizophrenia	NA	NA	NA	9		
Schizophreniform Disorder	NA	NA	NA	3		
Schizoaffective Disorder	NA	NA	NA	1		
Psychotic Disorder NOS	NA	NA	NA	13		
Brief Psychotic Disorder	NA	NA	NA	1		
Mood Disorders with psychotic symptoms	NA	NA	NA	4		
Delusional Disorder	NA	NA	NA	1		
Medication [e]**:** n (%)						
None	48 (100)	27 (71)	60 (52)	14 (44)		
Anti-depressants	0	11 (29)	46 (40)	14 (44)		
Mood stabilizers	0	0	5 (4)	0		
Anti-Psychotics	0	0	2 (2)	18 (56)		
Other	1 (2)	2 (5)	17 (15)	7 (22)		
MEG Trials: total included (SD)	88 (5.4)	87 (6.6)	86 (5.8)	83 (6.6)	H(3) = 14.9, p = 0.02	FEP < HC: p = 0.002
						FEP < CHR-N: p = 0.032
Task Performance						
Hit rate (% correct, SD)	99.6 (2.0)	99.2 (2.7)	99.5 (2.2)	98.1 (7.4)		
False Alarms (% errors, SD)	0.23 (1.03)	0.33 (0.79)	0.35 (0.82)	0.43 (0.74)		
Mean RT (ms, SD)	479 (97.5)	499 (122.9)	503 (129.2)	573 (192.0)		

Abbreviations: APS, attenuated psychotic symptoms; BACS, Brief Assessment of Cognition in Schizophrenia; CAARMS, Comprehensive Assessment of At Risk Mental States; COGDIS, Cognitive Disturbances, COGDIS, Cognitive-Perceptive Basic Symptoms criterion; HC, healthy controls; CC, clinical high risk negative clinical controls; CHR-P, clinical high risk positive; FEP, first-episode psychosis; GAF, global assessment of functioning; GF, global functioning; MINI, Mini-International Neuropsychiatric Interview; PANSS, Positive and Negative Symptom Scale; SPI-A, Schizophrenia Proneness Instrument, Adult version; SD, standard deviation of the mean; ms, milliseconds; RT, reaction time; NA, Not Assessed

[a] Except for 'sex' statistical testing, which are based on Chi-Square tests, all other tests are based on non-parametric Kruskal-Wallis H-tests: alpha=0.05, 2-sided, adjusted for ties, post-hoc Bonferroni-corrected for multiple comparisons.

[b] BACS scores for clinical groups were standardized to control group data, controlled for sex.

[c] GRFD stands for 'genetic risk and functional decline'.

[d] Multiple ratings possible for comorbidities.

[e] Multiple ratings possible.

Table 2. Linear Discriminant Analyses for classification of APS-persistence and psychosis transitioning based on neural 40-Hz ASSR and clinical data.

	APS-P (n=41) vs. APS-NP (n=37)	CHR-P-T (n=11) vs. CHR-P-NT (n=105)
Predictor variables	**ASSR** = RTHA **clinical** = GF-role, SPIA-severity	**ASSR** = RTHA **clinical** = GAF, GF-social
Wilks Lambda, Chi-square (df), p-value	**ASSR + clinical:** Wilks Lambda = 0.906 X^2 (2) = 7.37, p = 0.061 **ASSR only:** Wilks Lambda = 0.957 X^2 (1) = 3.34, p = 0.068 **Clinical only:** Wilks Lambda = 0.944 X^2 (2) = 4.34, p = 0.114	**ASSR + clinical:** Wilks Lambda = 0.925 X^2 (3) = 8.74, p = 0.033* **ASSR only:** Wilks Lambda = 0.958 X^2 (1) = 4.91, p = 0.027* **Clinical only:** Wilks Lambda = 0.962 X^2 (1) = 4.38, p = 0.112
Standardized Canonical Discriminant Function Coefficients (full model)	GF-role = 0.713 RTHA = 0.667 SPIA-severity = -0.228	RTHA = 0.716 GF-social = 0.447 GAF = 0.321
Classification accuracy and ROC-based AUC	**ASSR + clinical:** 51.4% APS-NP - 58.5% APS-P (55.1% overall correctly classified) AUC = 0.661 **ASSR only:** 48.6% APS-NP - 63.4% APS-P (56.4% overall correctly classified) AUC = 0.602 **CLINICAL only:** 56.8% APS-NP - 56.1% APS-P (56.4% overall correctly classified) AUC = 0.621	**ASSR + clinical:** 73.3% CHR-P-NT - 72.7% CHR-P-T (73.3% overall correctly classified) AUC = 0.827 **ASSR only:** 55.2% CHR-P-NT - 81.8% CHR-P-T (57.8% overall correctly classified) AUC = 0.739 **CLINICAL only:** 66.7% CHR-P-NT - 72.7% CHR-P-T (67.2% overall correctly classified) AUC = 0.732

*Significant ($p < 0.05$) after leave-one-out cross-validation.

Abbreviations: ASSR, Auditory Steady State Responses; APS, attenuated psychotic symptoms; APS-P, persistent symptoms within a one-year period, APS-NP, remitted from APS in one-year period; CHR-P, clinical high risk positive; CHR-P-T, transitioned to psychosis (within 36 months); CHR-P-NT, non-transitioned group; GAF, global assessment of functioning; GF, global functioning; SPI-A, Schizophrenia Proneness Instrument, Adult version; AUC, Area under the Receiver Operating Characteristic Curve (ROC).